atmosphere

MDPI

Article

Gathering Pipeline Methane Emissions in Utica Shale Using an Unmanned Aerial Vehicle and Ground-Based Mobile Sampling

Hugh Z. Li [1,*], Mumbi Mundia-Howe [2], Matthew D. Reeder [2] and Natalie J. Pekney [3]

1 Oak Ridge Institute for Science and Education, National Energy Technology Laboratory, Pittsburgh, PA 15236, USA
2 Leidos, National Energy Technology Laboratory, Pittsburgh, PA 15236, USA; Mumbi.Mundia-Howe@netl.doe.gov (M.M.-H.); Matthew.Reeder@netl.doe.gov (M.D.R.)
3 U.S. Department of Energy, National Energy Technology Laboratory, Pittsburgh, PA 15236, USA; Natalie.Pekney@netl.doe.gov
* Correspondence: Zhongju.Li@netl.doe.gov; Tel.: +1-412-386-6530

Received: 20 May 2020; Accepted: 1 July 2020; Published: 5 July 2020

Abstract: The United States Environmental Protection Agency Greenhouse Gas Inventory only recently updated the emission factors of natural gas gathering pipelines in April 2019 from the previous estimates based on a 1990s study of distribution pipelines. Additional measurements are needed from different basins for more accurate assessments of methane emissions from natural gas midstream industries and hence the overall climate implications of natural gas as the interim major energy source for the next decade. We conducted an unmanned aerial vehicle (UAV) survey and a ground-based vehicle sampling campaign targeting gathering pipeline systems in the Utica Shale from March to April in 2019. Out of 73 km of pipeline systems surveyed, we found no leaks on pipelines and two leaks on an accessory block valve with leak rates of 3.8 ± 0.4 and 7.6 ± 0.8 mg/s. The low leak frequency phenomenon was also observed in the only existing gathering pipeline study in Fayetteville Shale. The UAV sampling system facilitated ease of access, broadened the availability of pipelines for leak detection, and was estimated to detect methane leaks down to 0.07 g/s using Gaussian dispersion modeling. For future UAV surveys adopting similar instrument setup and dispersion models, we recommend arranging controlled release experiments first to understand the system's detection limit and choosing sampling days with steady and low wind speeds (2 m/s).

Keywords: natural gas; methane emissions; UAV; mobile sampling; Gaussian dispersion

1. Introduction

Methane is the main component (76 to 92%, vol%) of natural gas and the second most abundant greenhouse gas after carbon dioxide (CO_2) [1,2]. The combustion of natural gas produces less than half the CO_2 emitted from coal combustion, and the other combustion byproducts are mainly water [3]. With the recent technological advancement of horizontal drilling and hydraulic fracturing, the United States is experiencing a shale gas boom, with its annual dry natural gas production increased by 67 percent from 18 to 30 trillion cubic feet between 2005 and 2018 [4]. In 2017, the United States became a net natural gas exporter and natural gas is predicted to be the interim major energy source for the next decade [5,6]. Methane has a short atmospheric lifetime of 10 years compared to hundreds of years for CO_2 [7]. However, methane itself has a global warming potential 28-36 times more than that of CO_2 in a time horizon of 100 years [1]. According to Alvarez et al. [8], if the leak rates of methane in the natural gas supply chain were less than 3.2% of the total natural gas production, the utilization of natural gas would be a short-term mitigation approach for battling climate change and fulfilling the

Paris Agreement [9]. Thus, it is essential to accurately characterize methane emissions from different segments of the natural gas supply chain [10].

Natural gas gathering operations transport raw gas from production sites to processing plants or interstate transmission pipelines. Alverez et al. [10] suggested that the gathering system was responsible for around 1/5 of methane emissions from the whole natural gas supply chain. In the current United States Environment Protection Agency (EPA) greenhouse gas inventory (GHGI), emissions factors for gathering pipelines were only recently updated in April 2019 from previous estimates based on a 1996 EPA study of distribution pipelines [11]. New measurements of gathering pipelines from different basins would help improve inventory estimates.

Few studies directly characterize methane leaks from gathering pipelines [12]. To our knowledge, the only existing study, Zimmerle et al. [12], surveyed 96 km of gathering pipelines in Fayetteville Shale based on a ground-based mobile sampling platform and concluded that using emission factors from more recent studies of distribution pipelines would significantly underestimate gathering pipeline emissions. In the study, one underground pipeline leak contributed more than 80% of the total measured methane emissions from the gathering pipeline systems in Fayetteville Shale [12]. Aside from the policy implication of an accurate methane emission inventory, finding leaks from gathering pipelines helps avoid a loss of gas, monetary damages, and personal casualty loss [13].

Gathering pipeline systems are mainly composed of three parts: the pipeline, pig launcher, and block valve. Gatherings pipelines are the pipeline segments (1) between oil/gas wells to gathering compressor stations and processing plants and (2) connecting these facilities to transmission or distribution pipelines. The materials of pipelines can be plastic, stainless steel, bare steel, wrought iron, and cast iron. The cast and wrought iron pipelines were installed over 60 years ago and were later found to be vulnerable to corrosion. Pipelines more recently built are mostly plastic or stainless steel [13]. Gathering pipelines operate at pressures lower than transmission pipelines, typically at a range from 30 to 7720 kPa [14]. Since gathering pipelines are mainly transporting raw gas instead of the refined gas, pipeline operators perform pigging exercises to remove debris and deposits in the pipelines and clean the transported gas. Block valves are used for stopping or directing gas flows in pipelines.

Typical approaches to studying natural gas facilities include onsite measurements [15,16], ground-based mobile sampling [17–22], and aircraft-based sampling [23–25]. Ground-based mobile sampling is less expensive compared to aircraft campaigns and more efficient in quantifying site-level emissions relative to onsite measurements. Von Fischer et al. integrated a pipeline leak detection system with Google Street View vehicles (Google LLC, Menlo Park, CA, USA) to rapidly locate and quantify urban natural gas pipeline leaks [21].

The use of unmanned aerial vehicles (UAV, or drones) is a new promising approach for surveying natural gas pipelines [26,27] and sampling thermodynamic and chemical properties of planetary boundary layer [28–36]. This approach does not require personnel to step on the pipeline to measure gas leaks. It is much safer, and the main operation requirement is that the UAV should be within line of sight from the Federal Aviation Administration (FAA). Golston et al. [27] indicated that a UAV carrying methane sensors could observe small methane leaks down to 0.01 g/s (2 standard cubic feet per hour) when flying at an altitude below 10 m.

In this work, we utilized a UAV system and a ground-based mobile platform together to derive emission factors for current gathering pipeline systems in the Utica Shale from March to April in 2019. The paper is organized to (1) provide an overview of the UAV system and the ground-based mobile platform; (2) use Gaussian dispersion modeling to infer the smallest detectable leak size; and (3) discuss the relative strengths and weaknesses of different methane survey techniques (UAV vs. ground-based mobile van).

2. Methods

2.1. Access to Pipeline Location Data

A significant challenge to conducting gathering pipeline surveys is obtaining pipeline location data. The scarcity of available records of gathering pipeline locations is partially due to little or no regulation of gathering pipelines among different states. Gathering pipelines are mostly in rural areas as they transport raw gas from oil/gas wells [12]. We contacted the pipeline regulation agencies in Wyoming, Utah, New Mexico, and Oklahoma, and failed to obtain pipeline locations. These states' agencies might require a permit but do not hold inspection records or specific pipeline locations. However, the Public Utilities Commission (PUC) of Ohio regulates intrastate pipelines inside Ohio, including gathering pipelines constructed after 2012 due to the increase in the number of newer horizontally drilled and hydraulically fractured Utica and Marcellus Shale gas wells. The Utica Shale is located thousands of meters below the prolific Marcellus Shale and underlies most of Pennsylvania, Ohio, West Virginia, New York, and Quebec. The Utica and Marcellus regions have accounted for 85% of the increase in natural gas production in major U.S. oil/gas basins [4]. Ohio ranks sixth among all U.S. states in oil and gas producing capacities [4]. In 2018, Ohio's natural gas production was 28 times more than that in 2012 [4].

Natural gas companies are required to report to Ohio PUC accurate pipeline locations using ESRI shapefiles, Google Earth KML (Keyhole Markup Language), and/or PDFs. We used these files to contact several natural gas companies to request access to the pipeline rights-of-way for a ground-based survey.

We also purchased additional pipeline data products from Rextag (Hart Energy, Houston, TX, USA). This pipeline data included more pipelines than the PUC data and was not limited to those from newer horizontally drilled and hydraulically fractured wells.

2.2. UAV Setup and Flight Plan

UAV flights were conducted in eastern Ohio (Figure 1). SkySkopes (SkySkopes, Inc., Grand Forks, ND, USA) performed the UAV survey on nine separate days (03/22-03/30). The total flight time for the 53 flights was 12 h, during which 56 km of gathering pipelines were surveyed. Table 1 lists weather conditions and specific sampling distances on each UAV flight day.

Table 1. Overview of unmanned aerial vehicle (UAV) flights.

Date	Number of Flights	Weather	Distance Flown (km)
3/22/2019	4	Morning scattered rain with high winds in the afternoon	2.3
3/23/2019	9	Mostly sunny	5.1
3/24/2019	9	Mostly sunny	7.2
3/25/2019	0	Rain all day	0
3/26/2019	8	Sunny	7.4
3/27/2019	8	Sunny	10
3/28/2019	8	Partly cloudy	9.6
3/29/2019	5	Overcast, light winds	11.7
3/30/2019	2	Strong winds	2.3

The UAV is a Matrice 600 (DJI Technology Co., Ltd., China) with a payload capacity of 6 kg. It has a Mirage HC (Infrared Cameras Inc., Beaumont, TX, USA) optical gas imaging (OGI) camera and Tunable Diode Laser Absorption Spectrometer (TDLAS) methane sensor (Infrared Cameras Inc., Beaumont, TX, USA) on board. Both instruments have a power consumption less than 5 W. The OGI camera collects radiometric temperature data and produces thermal images using its 640 × 512 InSb array. The camera weighs less than 800 g. It can measure leaks of methane and other hydrocarbons larger than 2×10^{-4} g/s. The TDLAS measures methane absorption along an open path in the near-infrared region (laser wavelength 1650 nm). Based on Beer's law, the TDLAS reports methane concentration in ppm-m. Assuming methane is well mixed along a 1-m absorption path, the path integrated unit ppm-m is equal to the volume fraction of methane along the path. Since no dispersion characteristics

are known before the measurement is made, it is difficult to directly convert the ppm-m to commonly used ppm units. The TDLAS has a time resolution of 1 Hz and can measure methane from a distance up to 50 m with a resolution of 1 ppm-m. All instruments are synchronized before the campaign.

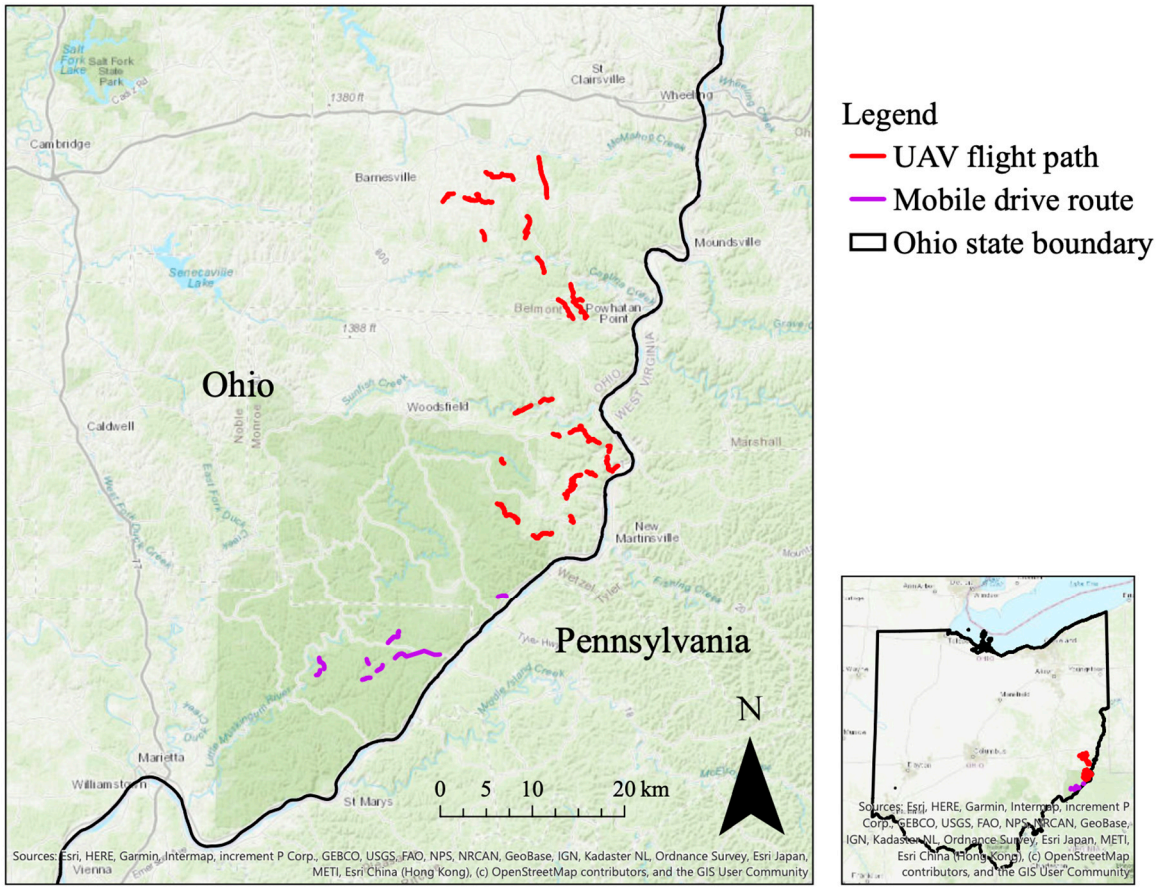

Figure 1. Overview of two survey paths (UAV and ground-based mobile sport utility vehicle (SUV)) in the Utica Shale, specifically in Ohio.

The factory recommended flight time for a Matrice 600 UAV is 20 minutes. For each flight, the range of the final flight time was from 10 to 20 minutes. The low end of the flight time was mainly due to the rough terrain in eastern Ohio (Figure S1, Supplemental Material) and line-of-sight requirements from the FAA. To create the flight paths, routes from the Google Earth app (Google LLC, Mountainview, CA, USA) were exported to KML files that were then imported to the Litchi software (VC Technology Ltd., London, UK). The Lichi app controlled the speed and altitude of the UAV remotely. The UAV could fly above the ground at user-defined heights regardless of the elevation of the terrain. The factory recommended flight height is between 40 and 50 m. The final range of flight heights was from 42 to 45 m.

The UAV would take off on flat ground and away from road traffic and obstacles, such as power lines (Figure 2). Each flight covered the selected pipeline segments twice, once in each direction. The average width of the pipelines' right-of-way was 10 m. The flight path was 6 m within the center of the pipelines at all times. The speed of the UAV ranged from 3.0 to 4.5 m/s. Since the TDLAS collected data in 1 Hz, the UAV collected a methane reading every 3 to 4.5 m.

We placed a portable weather station, 110-WS-25P-B (NovaLynx Corporation, Grass Valley, CA, USA), to collect ground wind speed and direction measurements in each sampling area. The weather station was secured on a tripod and measured winds at a height of 1.8 m above ground (Figure S2, Supplemental Material).

(a) (b)

Figure 2. (**a**) UAV and (**b**) ground-based sampling vehicle used in this study.

2.3. Ground-Based Vehicle Sampling Setup

A Ford Expedition sport utility vehicle (SUV) was used for the ground-based mobile survey on two trips (04/12/2019 and 04/16/2019). Note that the ground-based mobile survey happened after the UAV flights. In total, 17 km of above-ground pipelines were surveyed.

Although Ohio has 17,000 km of gathering pipelines in total, approximately 160 km are on public lands based on the purchased data products. The mobile survey was restricted to public lands (Wayne National Forest) due to the ease of access as compared to private property. This area of Ohio has rough terrain, with slope degrees frequently larger than 15 degrees (Figure S1, Supplemental Materials).

The details of the mobile sampling approach have been previously described [17]. The cargo area of the vehicle housed an LGR methane analyzer (Los Gatos Research LGR, CA, USA), a Windows laptop for logging data, and a power source for the instruments—a swappable 4–18 V Lithium-ion Bosch battery 6 Ah (Bosch, Blaichach, Germany). The A21™ ANTENNA GPS (Hemisphere GNSS, Scottsdale, AZ) was installed at the top center of the SUV. Wind speed and direction were measured by a weather station, Airmar 200WX, designed for mobile sampling (Airmar, Milford, NH, USA). The Airmar weather station was elevated by a polyvinyl chloride (PVC) pipe to a height of 2.5 m above the ground (Figure 2). This setup helped ensure wind measurements were not affected by vehicle movements [18,37–40]. Our sampling line was a 1/4" OD Teflon tube attached to the weather station. The LGR methane analyzer used an oil-free vacuum pump KNF N920 (KNF Neuberger, Inc., Trenton, NJ) for sample collection at a rate of 20 LPM. All instruments were secured so the effects of vehicle motion-induced vibration were minimized. All instruments were synchronized before the survey and reported data in local Eastern time (UTC/GMT-4).

Two researchers participated in each mobile sampling trip, a driver and a co-pilot. The co-pilot checked the analyzer's methane concentration readings for any elevation larger than 0.5 ppm above background 1.9 ppm [41]. We used methane readings at upwind rural locations as our background [42]. Since some of the pipelines in the forest were above ground, the co-pilot would also point a handhold methane detector, the Laser Methane Copter (LMC, Pergam Suisse AG, Switzerland), at the pipeline. When the co-pilot observed methane plume events as registered by the methane analyzer and indicated on the computer logging software, the driver would pull over and stop the vehicle so that the potential leak could be located. Once the leak was found, an infrared camera GF320 (FLIR Systems, Wilsonville, OR, USA) was mounted on a tripod to take infrared images and videos. We used the Bacharach Hi Flow® Sampler to quantify leak rates. Note the LGR methane analyzer provided methane concentrations but not methane leak rates. For each leak, both high and low flow modes (210 and 150 LPM) were used to get repeated leak rate measurements. Studies have shown that the Bacharach Hi Flow® Sampler could underestimate methane emissions due to the sensor failing to switch measurement modes [43]. In our

practice, we followed the recommendations of Connolly et al. [43], which included shutting down the Hi Flow sampler after measuring every single leak and conducting frequent calibration checks. It is unlikely that we were affected by this type of failure.

2.4. Data Quality Control

For the UAV sampling, weather conditions were examined using www.windy.com prior to each takeoff. Flights were cancelled or postponed if wind speeds were above 4.5 m/s because, at high winds, leaked methane would disperse rapidly, lowering the chances of detection. Rain and snow were also avoided, as the UAV and/or sensors could be damaged. During the UAV campaign (03/22 to 03/30), we observed rain on two days.

As there sometimes were discrepancies between the pipeline location in the Google Earth KML and the field-observed pipeline rights-of-way or markers, best judgment as to actual pipeline location was used to adjust the flight plan. Because the UAV flight paths were designed to pass over each segment of the route twice, any leak should be detected at approximately the same location during each pass. In addition, a ramping followed by a gradual decrease in methane concentration was expected to be observed as the UAV approached and then departed the leak location. We set the warning threshold of the TDLAS to be 200 ppm-m, an order of magnitude higher than background (Figure 3). If elevated, ramped-up methane concentration was observed twice around the same spot during one flight, a second flight would be conducted to collect additional data. The UAV would hover above the potential leaking spot, and then be lowered to the minimum allowable height to collect the thermal infrared output and to take videos that would allow for the examination of any vegetation degradation.

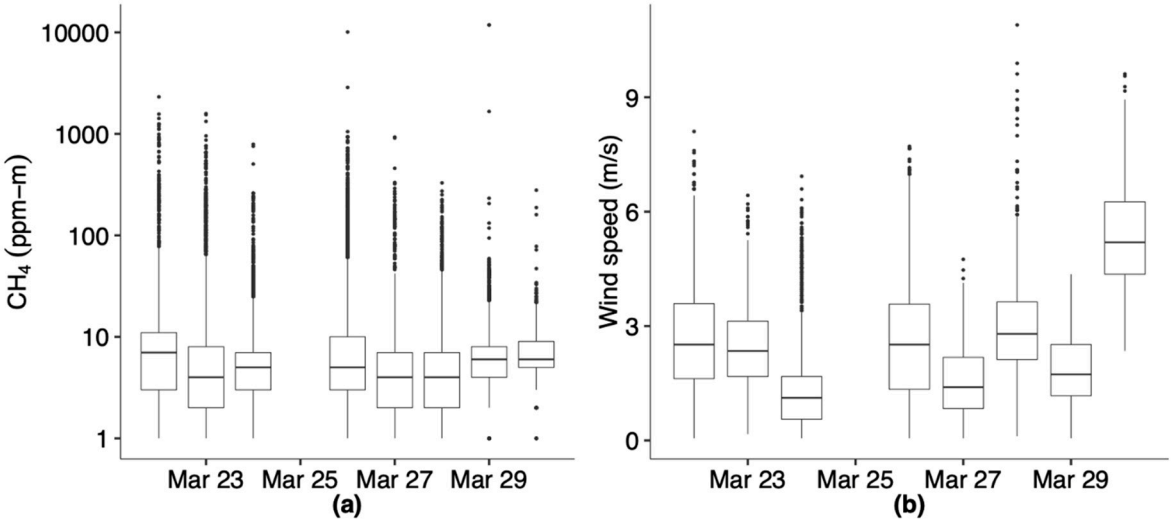

Figure 3. Boxplot of (**a**) methane readings and (**b**) wind speeds among all sampling days. The middle line is the median. The top and bottom of the box are the 75th and 25th percentiles. The outer whiskers extend to the most extreme values not yet classified as outliers [44]. The y axis for (**a**) is log scaled.

As per the manufacturer's recommendations, a two-point gas calibration was performed for the Bacharach Hi Flow® Sampler before each mobile sampling trip. The calibration gases were 2.5% methane, balance air and 99% methane, balance nitrogen (Heath Consultants, Houston, TX, USA). We chose these two gas compositions as they were included in the calibration menu of the Bacharach Hi Flow® Sampler.

For ground-based mobile sampling measurements, we filtered the methane dataset for null values and any methane values less than 1.5 ppm. The wind data from the Airmar 200 WX were adjusted based on the in-built data quality indicator. In addition, we conducted residence tests to measure

traveling time inside the sampling lines before the air samples reached the analyzer. This helped to better synchronize the GPS with the methane concentration data.

Calibration checks for the LGR methane analyzer were conducted as per manufacturer's recommendations. The cavity ring down spectroscopy-based analyzer showed good stability and little drift during field campaigns [17]. The calibration check results are in Table S1 (Supplemental Material). The analyzer showed good agreement (within 10%) with the methane reference standard (Accuracy: 2%, Matheson Tri-Gas, Inc., Bernards, NJ, USA).

2.5. Gaussian Dispersion Modeling

Gaussian dispersion modeling has been used in oil and gas research campaigns to quantify source emission rates [17,45]. Assuming a total reflecting ground for methane, a slender plume case, and the measurement takes place in the plume's center line, the simplified Gaussian model will be:

$$c(x, y = 0, z) = \frac{q}{2\pi\overline{u}\sigma_y\sigma_z} \times \left[exp\left(\frac{-(z-h)^2}{2\sigma_z^2} \right) + exp\left(\frac{-(z+h)^2}{2\sigma_z^2} \right) \right] \quad (1)$$

where c(x, y, z) is the methane concentration (g/m^3) in a specific location (x, y, z), q is the methane leak rate (g/s), $\overline{u}$ is the mean wind speed (m/s), σ_y, σ_z are the dispersion coefficients in the y, z direction (m), and h is the source releasing height above ground (m). We used the Pasquill–Gifford correlations to calculate the final dispersion coefficients [46].

2.6. Controlled Release Experiment

We conducted a controlled release experiment on 03/28/2019 to verify the leak detection ability of the methane sensors on the UAV. The weather was sunny, and the wind speeds averaged 4 m/s. We chose an open area for the experiment (Figure S2, Supplemental Materials). To simulate a pipeline leak, we used a 5% methane (vol%) cylinder (Matheson Tri-Gas, Inc., Irving, TX, USA, balance helium, certification accuracy 2%) releasing methane at a flow rate of 5 SLPM (standard liter per minute), as measured by an Alicat mass flow meter (Alicat Scientific, Tucson, AZ, USA). This flow rate was typical of leaks found on gathering and distribution pipelines [12,47]. Multiple flights were conducted with the cylinder valve closed or open. The operator flew the drone in the same way as was done for the actual pipeline survey.

3. Results and Discussion

The UAV surveyed 56 km of gathering pipelines and the ground-based SUV survey added another 17 km. The UAV surveyed pipelines were all stainless steel based on the Ohio PUC and Rextag data sources. The SUV surveyed 1 km of cast iron and 16 km of plastic pipelines. The diameters of the pipelines ranged from 2.5 to 61.0 cm.

3.1. TDLAS Minimum Detection Limit (MDL)

In our study, the UAV operator SkySkopes used a methane reading of 200 ppm-m as the indicator of a potential leak. The methane measurements from the UAV were about 4 m from the centerline of the pipeline on average. The releasing height for the underground pipeline leaks was at the ground level (z = 0 m). The survey area was mostly covered with trees. For a typical wind speed of 2.2 m/s (5 mph, Figure 3), our MDL was 0.07 g/s. This MDL is comparable to those reported in other studies. Subramanian et al. measured different components at compressor stations onsite and reported an MDL of 0.02 g/s [16]. Von Fischer et al. deployed instruments on Google Street View vehicles and focused on urban natural gas leaks within 20 m of the vehicle [21]. Their setup strategically dismissed small leaks and had an MDL of 0.5 g/s. Atherton et al. integrated methane analyzers on a mobile sampling platform and obtained an MDL of 0.06 g/s when they were sampling very close to the natural gas wells (<60 m) [45]. The MDL for this study was 20% larger compared to Atherton et al. at similar measuring

distances (tens of meters). This was due to their practice of resolving smaller methane peaks using ratio-based methods [45].

Throughout the controlled release experiment, the TDLAS on the UAV did not detect methane readings larger than 200 ppm-m at the typical survey flight height of 44 m. The OGI camera did not capture images or videos indicative of leaked methane as well due to the dilution of the leaked gas (5% vol. methane). According to the Gaussian inverse modeling and MDL results presented above, the TDLAS sensor on the UAV was able to detect a methane leak down to 0.07 g/s during ideal weather conditions (unstable atmosphere, constant wind). The gas releasing from the cylinder was simulating a pipeline leak with the smallest detectable leak rate at 0.07 g/s. The controlled release experiment demonstrated the added difficulty of methane leak detection in the real world [24]. The MDL calculation was only suggestive of the size of the detectable leaks in certain atmospheric conditions. The known issue with Gaussian dispersion modeling was the associated large uncertainty in final estimates due to atmospheric variability, wind speed, stability, plume turbulent diffusion, etc. [48]. The reference uncertainty range was from 50% to 350% [48]. Changing wind and weather conditions could greatly contribute to the fast dispersion of leaked methane and add difficulty of detecting the leak.

3.2. Low Pipeline Leak Frequency

Figure 3 shows the distribution of methane concentrations during the UAV survey. For all sampling days, methane background at 42–45 m above ground was around 8 ppm-m. Hundreds of methane readings were larger than the defined plume threshold of 200 ppm-m and were observed on all sampling days, with the largest methane reading more than 10,000 ppm-m. To eliminate false positives and outliers, we relied on a ramping curve of methane readings, the reoccurrence of the methane peak during both passes of the flight, and visual confirmation with the OGI camera during hovering to determine the existence of a methane leak. Single or few high methane readings were not necessarily good indications of pipeline leaks. During all 56 km of the UAV survey, we found six areas of interest with potential leaks. Separate flights were conducted to re-examine potential leaking spots, but we did not re-capture the high methane readings. Although the total size of collected data (methane analyzer logs, GPS, and infrared pictures/videos) was around 8 Gigabytes, most data did not show signs of pipeline leaks but plainly background methane concentrations.

Winds were relatively constant and mild during most of the sampling days (Figure 3b). The first seven sampling days had average wind speeds around 2.5 m/s. We experienced strong winds (>6 m/s) on the last sampling day (03/30/2019) and had to call off the sampling early.

During the ground-based mobile SUV survey, two methane leaks points were found on the same block valve located on a plastic pipeline (Figure S3A, Supplemental Materials). Leakage rates were 3.8 ± 0.4 and 7.6 ± 0.8 mg/s as measured by the high flow sampler. Based on the records kept in the Wayne National Forest Ranger's office, most of the gathering pipelines in the forest were plastic and above ground. When in need of crossing a trail or road, pipeline operators would hang the gas pipeline on the trees (Figure S3B, Supplemental Materials).

The low leak frequency (one leak found in a 73 km gathering pipeline system) in this study is similar to the results of Zimmerle et al. [12]: one leak of 1.1 g methane/s found in 96 km of pipelines. Pipeline age may be a factor that affects leakage rate. In the Fayetteville Shale region where the Zimmerle et al. study was conducted, more than 80% of active wells were drilled after 2008 [49]. In our Utica Shale sampling region, more than 67% of wells were drilled after 2000 and 70% of the gathering pipelines in this study were constructed after 2010 [50]. Newer pipelines generally do not leak unless there are installation flaws, accidental penetration, ground movement or other disruptions. In addition, the pipeline operators constructed these new gathering pipelines in a similar way as transmission pipelines with a rights-of-way width of 20 m on average. This carefully designed pipeline configuration also reduced the chance of leak incidences by facilitating easier inspections. As this study with mobile sampling was restricted to surveying on public roads, we could not drive the vehicle on

the pipeline rights-of-way easily due to the lengthy legal processing time in site access agreement. Therefore, it was difficult for the vast measurement of leaks from flanges, packing valves, and other above ground potential leak points. A recent study by Ulrich et al. describes the difficulty in detecting leaks from natural gas pipelines due to dispersion. When a methane leak (>80 vol%) emanated from the underground gas pipeline, its atmospheric concentration would drop to 10–100 ppm within 10 cm above the surface when the wind speed was more than 2 m/s [51].

4. Conclusions

We surveyed 73 km of gathering pipelines (56 km from the UAV, 17 km from the ground-based mobile SUV) and found two leaks on the same block valve. This low leak frequency made it difficult to refine the emission factors of gathering pipelines in this region. As we would conduct similar gathering pipeline studies in other basins in the near future, we would eventually sample diverse gathering pipelines in different basins and provide data for new emission factor calculation.

The UAV platform can be used to survey previously inaccessible pipelines due to rough terrain (Figure S1, supplemental materials). The whole logistics will be cheaper compared to a manned aircraft. The UAV is also highly customizable. The flight pattern can be fairly close to ground [52] or up to 1 km above the ground level [53]. With the continuing development of the UAV industry and the sensor technology, in the foreseeable future, the application of UAVs in monitoring oil and gas infrastructure is promising. In our campaign, most of the pipelines were surveyed by the UAV platform (56 km out of 73 km). The pipelines did not have good access roads, and a flexible SUV platform could not be utilized to survey these types of pipelines. Again, the comparison here highlights the benefits of using UAVs in surveying natural gas pipelines, especially for the gathering pipelines commonly found in rural or remote areas. Another added benefit of the UAV platform is that the operating personal does not need to step on the pipelines, thus minimizing the risk of damages due to pipeline explosion or airborne pollutants exposure, such as volatile organic compounds [54–59]. Ground-based mobile sampling is also highly customizable and comparably less expensive to implement compared to the UAV platform. Various state of the art instruments can be deployed with proven accuracy/precision in previous field studies. However, the terrain is a limiting factor for ground-based mobile sampling, as seen in our study.

The ideal situation for a UAV pipeline survey project would be willing partners to provide pipeline location and site access, flat terrain, and good weather conditions with constant wind direction and low wind speeds (2 m/s). For future gathering pipeline studies, we recommend conducting control release experiments to verify the detection limits of the pipeline leak detection system first.

Supplementary Materials: The following are available online at http://www.mdpi.com/2073-4433/11/7/716/s1, Figure S1: Slope map of the sampling areas' terrain in Ohio. Figure S2: Portable weather station used to measure ground wind speed and direction. Figure S3: (**A**) Methane leaks from the two screws on the gathering pipeline accessories. (**B**) Black plastic gathering pipelines were hanging over the trees to cross the road. Table S1: Calibration check results for the LGR analyzer.

Author Contributions: Conceptualization, H.Z.L., M.M.-H. and N.J.P.; Data curation, H.L.L., M.M.-H., M.D.R. and N.J.P.; Formal analysis, H.Z.L.; Investigation, H.Z.L., M.M.-H. and N.J.P.; Methodology, H.Z.L., M.M.-H. and M.D.R.; Project administration, N.J.P.; Resources, N.J.P.; Supervision, N.J.P.; Validation, H.Z.L.; Visualization, H.Z.L.; Writing—original draft, H.Z.L.; Writing—review & editing, H.Z.L. and N.J.P. All authors have read and agreed to the published version of the manuscript.

Funding: This research received no external funding.

Acknowledgments: This technical effort was performed in support of the National Energy Technology Laboratory's ongoing research under Natural Gas Infrastructure Field Work Proposal DOE 1022424. This report was prepared as an account of work sponsored by an agency of the United States Government. Neither the United States Government nor any agency thereof, nor any of their employees, makes any warranty, express or implied, or assumes any legal liability or responsibility for the accuracy, completeness, or usefulness of any information, apparatus, product, or process disclosed, or represents that its use would not infringe privately owned rights. Reference therein to any specific commercial product, process, or service by trade name, trademark, manufacturer, or otherwise does not necessarily constitute or imply its endorsement, recommendation, or favoring by the United States Government or any agency thereof. The views and opinions of authors expressed therein do not necessarily

state or reflect those of the United States Government or any agency thereof. Hugh Z. Li was supported in part by an appointment to the Science Education Programs at National Energy Technology Laboratory (NETL), administered by ORAU through the U.S. Department of Energy Oak Ridge Institute for Science and Education.

Conflicts of Interest: The authors declare no conflict of interest.

References

1. IPCC. Anthropogenic and Natural Radiative Forcing. In *Climate Change 2013—The Physical Science Basis: Working Group I Contribution to the Fifth Assessment Report of the Intergovernmental Panel on Climate Change*; Cambridge University Press: Cambridge, UK, 2014; pp. 659–740, ISBN 978-1-107-05799-9.
2. US EPA Inventory of U.S. Greenhouse Gas Emissions and Sinks. Available online: https://www.epa.gov/ghgemissions/inventory-us-greenhouse-gas-emissions-and-sinks (accessed on 12 February 2019).
3. EIA. EIA Carbon Dioxide Emissions Coefficients. Available online: https://www.eia.gov/environment/emissions/co2_vol_mass.php (accessed on 12 February 2019).
4. EIA U.S. Dry Natural Gas Production (Million Cubic Feet). Available online: https://www.eia.gov/dnav/ng/hist/n9070us2A.htm (accessed on 3 July 2019).
5. EIA. EIA Annual Energy Outlook. Available online: https://www.eia.gov/outlooks/aeo/ (accessed on 11 January 2019).
6. EIA Natural Gas Imports and Exports—Energy Explained, Your Guide to Understanding Energy—Energy Information Administration. Available online: https://www.eia.gov/energyexplained/index.php?page=natural_gas_imports (accessed on 3 July 2019).
7. Voulgarakis, A.; Naik, V.; Lamarque, J.-F.; Shindell, D.T.; Young, P.J.; Prather, M.J.; Wild, O.; Field, R.D.; Bergmann, D.; Cameron-Smith, P.; et al. Analysis of present day and future OH and methane lifetime in the ACCMIP simulations. *Atmos. Chem. Phys.* **2013**, *13*, 2563–2587. [CrossRef]
8. Alvarez, R.A.; Pacala, S.W.; Winebrake, J.J.; Chameides, W.L.; Hamburg, S.P. Greater focus needed on methane leakage from natural gas infrastructure. *Proc. Natl. Acad. Sci. USA* **2012**, *109*, 6435–6440. [CrossRef] [PubMed]
9. UNFCCC. The Paris Agreement|UNFCCC. Available online: https://unfccc.int/process-and-meetings/the-paris-agreement/the-paris-agreement (accessed on 24 June 2020).
10. Alvarez, R.A.; Zavala-Araiza, D.; Lyon, D.R.; Allen, D.T.; Barkley, Z.R.; Brandt, A.R.; Davis, K.J.; Herndon, S.C.; Jacob, D.J.; Karion, A.; et al. Assessment of methane emissions from the U.S. oil and gas supply chain. *Science* **2018**, eaar7204. [CrossRef] [PubMed]
11. Campbell, L.M.; Campbell, M.V.; Epperson, D.L. Methane Emissions from the Natural Gas Industry. *Undergr. Pipelines* **1996**, *9*, 100.
12. Zimmerle, D.J.; Pickering, C.K.; Bell, C.S.; Heath, G.A.; Nummedal, D.; Pétron, G.; Vaughn, T.L. Gathering pipeline methane emissions in Fayetteville shale pipelines and scoping guidelines for future pipeline measurement campaigns. *Elem. Sci. Anthr.* **2017**, *5*, 70. [CrossRef]
13. PHMSA. Pipeline Incident 20 Year Trends. Available online: https://www.phmsa.dot.gov/data-and-statistics/pipeline/pipeline-incident-20-year-trends (accessed on 29 January 2019).
14. Mitchell, A.L.; Tkacik, D.S.; Roscioli, J.R.; Herndon, S.C.; Yacovitch, T.I.; Martinez, D.M.; Vaughn, T.L.; Williams, L.L.; Sullivan, M.R.; Floerchinger, C.; et al. Measurements of Methane Emissions from Natural Gas Gathering Facilities and Processing Plants: Measurement Results. *Environ. Sci. Technol.* **2015**, *49*, 3219–3227. [CrossRef]
15. Luck, B.; Zimmerle, D.; Vaughn, T.; Lauderdale, T.; Keen, K.; Harrison, M.; Marchese, A.J.; Williams, L.L.; Allen, D.T. Multi-day Measurements of Pneumatic Controller Emissions Reveal Frequency of Abnormal Emissions Behavior at Natural Gas Gathering Stations. *Environ. Sci. Technol. Lett.* **2019**. [CrossRef]
16. Subramanian, R.; Williams, L.L.; Vaughn, T.L.; Zimmerle, D.; Roscioli, J.R.; Herndon, S.C.; Yacovitch, T.I.; Floerchinger, C.; Tkacik, D.S.; Mitchell, A.L.; et al. Methane Emissions from Natural Gas Compressor Stations in the Transmission and Storage Sector: Measurements and Comparisons with the EPA Greenhouse Gas Reporting Program Protocol. *Environ. Sci. Technol.* **2015**, *49*, 3252–3261. [CrossRef]
17. Li, H.Z.; Reeder, M.D.; Litten, J.; Pekney, N.J. Identifying under-characterized atmospheric methane emission sources in Western Maryland. *Atmos. Environ.* **2019**, 117053. [CrossRef]

18. Li, H.Z.; Dallmann, T.R.; Li, X.; Gu, P.; Presto, A.A. Urban Organic Aerosol Exposure: Spatial Variations in Composition and Source Impacts. *Environ. Sci. Technol.* **2017**. [CrossRef]
19. Omara, M.; Zimmerman, N.; Sullivan, M.R.; Li, X.; Ellis, A.; Cesa, R.; Subramanian, R.; Presto, A.A.; Robinson, A.L. Methane Emissions from Natural Gas Production Sites in the United States: Data Synthesis and National Estimate. *Environ. Sci. Technol.* **2018**, *52*, 12915–12925. [CrossRef] [PubMed]
20. Omara, M.; Sullivan, M.R.; Li, X.; Subramanian, R.; Robinson, A.L.; Presto, A.A. Methane Emissions from Conventional and Unconventional Natural Gas Production Sites in the Marcellus Shale Basin. *Environ. Sci. Technol.* **2016**, *50*, 2099–2107. [CrossRef] [PubMed]
21. von Fischer, J.C.; Cooley, D.; Chamberlain, S.; Gaylord, A.; Griebenow, C.J.; Hamburg, S.P.; Salo, J.; Schumacher, R.; Theobald, D.; Ham, J. Rapid, Vehicle-Based Identification of Location and Magnitude of Urban Natural Gas Pipeline Leaks. *Environ. Sci. Technol.* **2017**, *51*, 4091–4099. [CrossRef] [PubMed]
22. Ye, Q.; Gu, P.; Li, H.Z.; Robinson, E.S.; Lipsky, E.; Kaltsonoudis, C.; Lee, A.K.Y.; Apte, J.S.; Robinson, A.L.; Sullivan, R.C.; et al. Spatial Variability of Sources and Mixing State of Atmospheric Particles in a Metropolitan Area. *Environ. Sci. Technol.* **2018**, *52*, 6807–6815. [CrossRef]
23. Ren, X.; Salmon, O.E.; Hansford, J.R.; Ahn, D.; Hall, D.; Benish, S.E.; Stratton, P.R.; He, H.; Sahu, S.; Grimes, C.; et al. Methane Emissions From the Baltimore-Washington Area Based on Airborne Observations: Comparison to Emissions Inventories. *J. Geophys. Res. Atmos.* **2018**, *123*, 8869–8882. [CrossRef]
24. Cui, Y.Y.; Henze, D.K.; Brioude, J.; Angevine, W.M.; Liu, Z.; Bousserez, N.; Guerrette, J.; McKeen, S.A.; Peischl, J.; Yuan, B.; et al. Inversion Estimates of Lognormally Distributed Methane Emission Rates From the Haynesville-Bossier Oil and Gas Production Region Using Airborne Measurements. *J. Geophys. Res. Atmos.* **2019**, *124*, 3520–3531. [CrossRef]
25. Vaughn, T.L.; Bell, C.S.; Pickering, C.K.; Schwietzke, S.; Heath, G.A.; Pétron, G.; Zimmerle, D.J.; Schnell, R.C.; Nummedal, D. Temporal variability largely explains top-down/bottom-up difference in methane emission estimates from a natural gas production region. *Proc. Natl. Acad. Sci. USA* **2018**, *115*, 11712–11717. [CrossRef]
26. Yang, S.; Talbot, R.; Frish, M.; Golston, L.; Aubut, N.; Zondlo, M.; Gretencord, C.; McSpiritt, J. Natural Gas Fugitive Leak Detection Using an Unmanned Aerial Vehicle: Measurement System Description and Mass Balance Approach. *Atmosphere* **2018**, *9*, 383. [CrossRef]
27. Golston, L.; Aubut, N.; Frish, M.; Yang, S.; Talbot, R.; Gretencord, C.; McSpiritt, J.; Zondlo, M. Natural Gas Fugitive Leak Detection Using an Unmanned Aerial Vehicle: Localization and Quantification of Emission Rate. *Atmosphere* **2018**, *9*, 333. [CrossRef]
28. Barbieri, L.; Kral, S.; Bailey, S.; Frazier, A.; Jacob, J.; Reuder, J.; Brus, D.; Chilson, P.; Crick, C.; Detweiler, C.; et al. Intercomparison of Small Unmanned Aircraft System (sUAS) Measurements for Atmospheric Science during the LAPSE-RATE Campaign. *Sensors* **2019**, *19*, 2179. [CrossRef]
29. Lee, T.; Buban, M.; Dumas, E.; Baker, C. On the Use of Rotary-Wing Aircraft to Sample Near-Surface Thermodynamic Fields: Results from Recent Field Campaigns. *Sensors* **2018**, *19*, 10. [CrossRef] [PubMed]
30. Nolan, P.; McClelland, H.; Woolsey, C.; Ross, S. A Method for Detecting Atmospheric Lagrangian Coherent Structures Using a Single Fixed-Wing Unmanned Aircraft System. *Sensors* **2019**, *19*, 1607. [CrossRef] [PubMed]
31. Rautenberg, A.; Graf, M.; Wildmann, N.; Platis, A.; Bange, J. Reviewing Wind Measurement Approaches for Fixed-Wing Unmanned Aircraft. *Atmosphere* **2018**, *9*, 422. [CrossRef]
32. Rautenberg, A.; Schön, M.; Zum Berge, K.; Mauz, M.; Manz, P.; Platis, A.; van Kesteren, B.; Suomi, I.; Kral, S.T.; Bange, J. The Multi-Purpose Airborne Sensor Carrier MASC-3 for Wind and Turbulence Measurements in the Atmospheric Boundary Layer. *Sensors* **2019**, *19*, 2292. [CrossRef]
33. Schuyler, T.; Guzman, M. Unmanned Aerial Systems for Monitoring Trace Tropospheric Gases. *Atmosphere* **2017**, *8*, 206. [CrossRef]
34. Schuyler, T.J.; Bailey, S.C.C.; Guzman, M.I. Monitoring Tropospheric Gases with Small Unmanned Aerial Systems (sUAS) during the Second CLOUDMAP Flight Campaign. *Atmosphere* **2019**, *10*, 434. [CrossRef]
35. Schuyler, T.J.; Gohari, S.M.I.; Pundsack, G.; Berchoff, D.; Guzman, M.I. Using a Balloon-Launched Unmanned Glider to Validate Real-Time WRF Modeling. *Sensors* **2019**, *19*, 1914. [CrossRef]
36. Witte, B.; Singler, R.; Bailey, S. Development of an Unmanned Aerial Vehicle for the Measurement of Turbulence in the Atmospheric Boundary Layer. *Atmosphere* **2017**, *8*, 195. [CrossRef]

37. Gu, P.; Li, H.Z.; Ye, Q.; Robinson, E.S.; Apte, J.S.; Robinson, A.L.; Presto, A.A. Intracity Variability of Particulate Matter Exposure Is Driven by Carbonaceous Sources and Correlated with Land-Use Variables. *Environ. Sci. Technol.* **2018**, *52*, 11545–11554. [CrossRef]
38. Li, H.Z.; Gu, P.; Ye, Q.; Zimmerman, N.; Robinson, E.S.; Subramanian, R.; Apte, J.S.; Robinson, A.L.; Presto, A.A. Spatially dense air pollutant sampling: Implications of spatial variability on the representativeness of stationary air pollutant monitors. *Atmos. Environ. X* **2019**, 100012. [CrossRef]
39. Li, H.Z.; Dallmann, T.R.; Gu, P.; Presto, A.A. Application of mobile sampling to investigate spatial variation in fine particle composition. *Atmos. Environ.* **2016**, *142*, 71–82. [CrossRef]
40. Robinson, E.S.; Gu, P.; Ye, Q.; Li, H.Z.; Shah, R.U.; Apte, J.S.; Robinson, A.L.; Presto, A.A. Restaurant Impacts on Outdoor Air Quality: Elevated Organic Aerosol Mass from Restaurant Cooking with Neighborhood-Scale Plume Extents. *Environ. Sci. Technol.* **2018**. [CrossRef]
41. Phillips, N.G.; Ackley, R.; Crosson, E.R.; Down, A.; Hutyra, L.R.; Brondfield, M.; Karr, J.D.; Zhao, K.; Jackson, R.B. Mapping urban pipeline leaks: Methane leaks across Boston. *Environ. Pollut.* **2013**, *173*, 1–4. [CrossRef] [PubMed]
42. Saha, P.K.; Zimmerman, N.; Malings, C.; Hauryliuk, A.; Li, Z.; Snell, L.; Subramanian, R.; Lipsky, E.; Apte, J.S.; Robinson, A.L.; et al. Quantifying high-resolution spatial variations and local source impacts of urban ultrafine particle concentrations. *Sci. Total Environ.* **2019**, *655*, 473–481. [CrossRef] [PubMed]
43. Connolly, J.I.; Robinson, R.A.; Gardiner, T.D. Assessment of the Bacharach Hi Flow® Sampler characteristics and potential failure modes when measuring methane emissions. *Measurement* **2019**, *145*, 226–233. [CrossRef]
44. McGill, R.; Tukey, J.W.; Larsen, W.A. Variations of Box Plots. *Am. Stat.* **1978**, *32*, 12. [CrossRef]
45. Atherton, E.; Risk, D.; Fougère, C.; Lavoie, M.; Marshall, A.; Werring, J.; Williams, J.P.; Minions, C. Mobile measurement of methane emissions from natural gas developments in northeastern British Columbia, Canada. *Atmos. Chem. Phys.* **2017**, *17*, 12405–12420. [CrossRef]
46. Turner, D.B. *Workbook of Atmospheric Dispersion Estimates: An Introduction to Dispersion Modeling, Second Edition*; CRC Press: Boca Raton, FL, USA, 1994; ISBN 978-1-56670-023-8.
47. Lamb, B.K.; Edburg, S.L.; Ferrara, T.W.; Howard, T.; Harrison, M.R.; Kolb, C.E.; Townsend-Small, A.; Dyck, W.; Possolo, A.; Whetstone, J.R. Direct Measurements Show Decreasing Methane Emissions from Natural Gas Local Distribution Systems in the United States. *Environ. Sci. Technol.* **2015**, *49*, 5161–5169. [CrossRef]
48. Caulton, D.R.; Li, Q.; Bou-Zeid, E.; Fitts, J.P.; Golston, L.M.; Pan, D.; Lu, J.; Lane, H.M.; Buchholz, B.; Guo, X.; et al. Quantifying uncertainties from mobile-laboratory-derived emissions of well pads using inverse Gaussian methods. *Atmos. Chem. Phys.* **2018**, *18*, 15145–15168. [CrossRef]
49. AOGC. 2018 Arkansas Production & Well Data. Available online: http://www.aogc2.state.ar.us/welldata/default.aspx (accessed on 5 July 2019).
50. Ohio DNR Ohio Oil & Gas Well Production Numbers. Available online: http://oilandgas.ohiodnr.gov/production#COMB (accessed on 5 July 2019).
51. Ulrich, B.A.; Mitton, M.; Lachenmeyer, E.; Hecobian, A.; Zimmerle, D.; Smits, K.M. Natural Gas Emissions from Underground Pipelines and Implications for Leak Detection. *Environ. Sci. Technol. Lett.* **2019**. [CrossRef]
52. Nolan, P.; Pinto, J.; González-Rocha, J.; Jensen, A.; Vezzi, C.; Bailey, S.; de Boer, G.; Diehl, C.; Laurence, R.; Powers, C.; et al. Coordinated Unmanned Aircraft System (UAS) and Ground-Based Weather Measurements to Predict Lagrangian Coherent Structures (LCSs). *Sensors* **2018**, *18*, 4448. [CrossRef] [PubMed]
53. Alaoui-Sosse, S.; Durand, P.; Medina, P.; Pastor, P.; Lothon, M.; Cernov, I. OVLI-TA: An Unmanned Aerial System for Measuring Profiles and Turbulence in the Atmospheric Boundary Layer. *Sensors* **2019**, *19*, 581. [CrossRef] [PubMed]
54. Li, H.Z.; Reeder, M.D.; Pekney, N.J. Quantifying source contributions of volatile organic compounds under hydraulic fracking moratorium. *Sci. Total Environ.* **2020**, 139322. [CrossRef] [PubMed]
55. Gu, P.; Dallmann, T.R.; Li, H.Z.; Tan, Y.; Presto, A.A. Quantifying Urban Spatial Variations of Anthropogenic VOC Concentrations and Source Contributions with a Mobile Sampling Platform. *Int. J. Environ. Res. Public. Health* **2019**, *16*, 1632. [CrossRef]
56. Shah, R.U.; Coggon, M.M.; Gkatzelis, G.I.; McDonald, B.C.; Tasoglou, A.; Huber, H.; Gilman, J.; Warneke, C.; Robinson, A.L.; Presto, A.A. Urban Oxidation Flow Reactor Measurements Reveal Significant Secondary Organic Aerosol Contributions from Volatile Emissions of Emerging Importance. *Environ. Sci. Technol.* **2020**, acs.est.9b06531. [CrossRef] [PubMed]

57. Ye, Q.; Li, H.Z.; Gu, P.; Robinson, E.S.; Apte, J.S.; Sullivan, R.C.; Robinson, A.L.; Donahue, N.M.; Presto, A.A. Moving beyond Fine Particle Mass: High-Spatial Resolution Exposure to Source-Resolved Atmospheric Particle Number and Chemical Mixing State. *Environ. Health Perspect.* **2020**, *128*, 017009. [CrossRef]
58. Donahue, N.M.; Posner, L.N.; Westervelt, D.M.; Li, Z.; Shrivastava, M.; Presto, A.A.; Sullivan, R.C.; Adams, P.J.; Pandis, S.N.; Robinson, A.L. Where Did This Particle Come From? Sources of Particle Number and Mass for Human Exposure Estimates. In *Issues in Environmental Science and Technology*; Harrison, R.M., Hester, R.E., Querol, X., Eds.; Royal Society of Chemistry: Cambridge, UK, 2016; pp. 35–71, ISBN 978-1-78262-491-2.
59. Robinson, E.S.; Shah, R.U.; Messier, K.; Gu, P.; Li, H.Z.; Apte, J.S.; Robinson, A.L.; Presto, A.A. Land-Use Regression Modeling of Source-Resolved Fine Particulate Matter Components from Mobile Sampling. *Environ. Sci. Technol.* **2019**, *53*, 8925–8937. [CrossRef]